On the dissolution rate on nanomaterials determined by ions and by particle size under lysosomal conditions: contributions to standardisation of simulant fluids and analytical methods.

Ilaria Zanoni [L], Johannes G. Keller[†‡], Ursula G. Sauer[J], Philipp Müller[†], Lan Ma-Hock[‡], Keld A. Jensen [Ⱶ], Anna Luisa Costa [L], Wendel Wohlleben[†‡*]

† BASF SE, Dept. of Material Physics and Analytics, 67056 Ludwigshafen, Germany

[L] CNR-ISTEC-National Research Council of Italy, Institute of Science and Technology for Ceramics, 48018, Faenza, Italy

[J] Scientific Consultancy - Animal Welfare, 85579 Neubiberg, Germany

[Ⱶ] National Research Centre for Work Environment (NRCWE), 2100 Copenhagen, Denmark

‡ BASF SE, Dept. of Experimental Toxicology and Ecology, 67056 Ludwigshafen, Germany

* Corresponding author: wendel.wohlleben@basf.com;

BASF SE, Carl-Bosch-Strasse, Building B7, 67056 Ludwigshafen, Germany

Supporting Information

Details on the literature review, simulant media composition and TEM images of SiO_2 and CeO_2.

Details on the literature review:

The following queries were conducted in December 2018 and January 2019 in the US National Institutes of Health National Library of Medicine database PubMed [1] to search for literature informing on the specific composition of macrophage lysosomes:

1. *lysosom* (morpholog* OR compos*) macrophage* = 944 retrievals on 18 January 2019.

To reduce the total number of retrievals, the following restriction was applied:

2. *lysosom* (morpholog* OR compos*) macrophage (alveol* OR lung OR pulmonary) = 142 retrievals on 18 January 2019;

3. *lysosom* (morpholog* OR compos*) macrophage[ti] = 69 retrievals on 18 January 2019;

4. *lysosom*[ti] (morpholog* OR compos*) macrophage = 103 retrievals on 18 January 2019.

All titles and abstracts retrieved via search queries 2-4 were evaluated for potential relevance of the publication to inform on macrophage lysosome composition. Potentially relevant publications were evaluated in full text. Additionally, the references in these publications (and in the publications addressing MMVF or nanomaterial dissolution rate of) were checked for potential relevance.

Table SI_1: Composition of pH 4.5 extraction fluids reported in the literature (g/L; unless otherwise noted), reproduced from Sauer et al. (2021) [2]. (Reproduced from Sauer, U. G.; Werle, K.; Waindok, H.; Hirth, S.; Hachmöller, O.; Wohlleben, W. Critical Choices in Predicting Stone Wool Biodurability: Lysosomal Fluid Compositions and Binder Effects. Chem. Res. Toxicol. 2021. Copyright 2021 American Chemical Society.)

| | Christensen et al. (1994) | Thélohan & de Meringo | Guldberg et al. (1998) | | | | | Muhle et al. (1998) | Stopford et al. (2003) | Stefaniak et al. (2005) | | Midander et al. (2007) | Shinohara et al. (2017) |
			A: MK (HCl)	B: MG (HCl)	C: MK (phthalate)	D: MG (citrate)	E: MG (HCl)			"PSF"	B&A		
MgCl₂ * 6 H₂0	0.212	0.106		0.212		0.106	0.160	0.106	0.106		4.615		0.142
MgCl₂												0.0497	
NaCl	7.120	3.210	6.780	7.120	6.650	3.208	6.171	3.208	3.210	6.650	2.01	3.210	4.200
NaOH		6				1.888			6			6.000	8.000
KCl							0.031				8.700		
CaCl₂	-	0.097	0.022										0.130
CaCl₂ * 4 H₂O								0.159					
CaCl₂ * 2 H₂O	0.029			0.029	0.029	0.128	0.060			0.029	0.765	0.128	
NH₄Cl			0.536		0.535								
H₂SO₄			0.196										
Na₂SO₄ (anhydrous)	0.079	0.039		0.079	0.071	0.040	0.080		0.039	0.071		0.039	0.052
Na₂SO₄ * 10 H₂O								0.090					
Na₂HPO₄	0.148			0.148	0.171	0.074	0.148	0.074		0.142		0.071	
Na₂HPO₄ * 12 H₂O	-	0.179											
Na2HPO4 * 7 H₂O										0.179			0.240
NaH₂PO₄			0.141										
NaHCO₃	1.950		2.268	1.950			1.900						
NaCH₃CO₂ * 3 H₂0					0.954								
Na₂-tartrate * 2 H₂O	0.180	0.090		0.18		0.090	0.180	0.090	0.090			0.090	0.120
Citric acid		20.800							20.800			20.800	28.000
Citric acid * H₂O						5.424			0.128				
Na₃-citrate			0.051										
Na₃-citrate * 2 H₂O	0.152	0.077		0.152	0.059	0.076	0.152	5.313	0.077			0.077	0.102
90% lactic acid	0.156			0.14		0.079	0.056						
Na-lactate		0.085						0.088	0.085			0.085	0.220
Glycine	0.118	0.059	0.454	0.118	0.45	0.059	0.118	0.059		0.450	0.450	0.059	
Glycerine									0.059				0.078
KH-phthalate					2.043					4.085	4.086		

S3

	Christensen et al. (1994)	Thélohan & de Meringo	Guldberg et al. (1998)					Muhle et al. (1998)	Stopford et al. (2003)	Stefaniak et al. (2005)		Midander et al. (2007)	Shinohara et al. (2017)
			A: MK (HCl)	B: MG (HCl)	C: MK (phthalate)	D: MG (citrate)	E: MG (HCl)			"PSF"	B&A		
Na-pyruvate	0.172	0.086		0.172		0.086	0.172	0.086	0.086			0.086	0.114
Benzalconium-Cl										50 ppm			
Formalin	1 mL	1 ml/L						1 mL					3.8
HCl	3.7 mL/L		0.78	750			0.881						

Abbreviations to Table 2: B&A: Baron and Ahmed solution of leukocyte intracellular fluid; MG: Modified Gamble's solution; MK: Modified Kanapilly; PSF: Phagolysosomal simulant fluid.

S4

Table SI_2: Physico-chemical characteristics of TiO_2, ZnO, SiO_2, $BaSO_4$ and CeO_2 ENMs. Characterisation techniques are abbreviated, in order of appearance, as follows: CAS: Chemical Abstracts Service, XRD: X-Ray Diffraction, XRF: X-Ray Fluorescence, TEM: Transmission Electron Microscopy, BET: Brunauer–Emmett–Teller, XPS: X-Ray Photoelectron Spectroscopy, FRAS: Ferric Reduction Ability of Serum, EPR: Electron Paramagnetic Resonance Spectroscopy, DMPO: 5,5-Dimethyl-1-pyrroline-N-oxide, CPH: 1-hydroxy-3-carboxy-pyrrolidine and REACH: Registration, Evaluation, Authorisation and Restriction of Chemicals. This table is equally used by Llewellyn et al (2021) [3]. (Adapted with permission from Llewellyn, S. V.; Conway, G. E.; Zanoni, I.; Jørgensen, A. K.; Shah, U. K.; Seleci, D. A.; Keller, J. G.; Kim, J. W.; Wohlleben, W.; Jensen, K. A.; Costa, A.; Jenkins, G. J. S.; Clift, M. J. D.; Doak, S. H. Understanding the Impact of More Realistic Low-Dose, Prolonged Engineered Nanomaterial Exposure on Genotoxicity Using 3D Models of the Human Liver. J. Nanobiotechnology 2021, 19 (1), 1–24. Copyright 2021 BioMed Central.)

ENM Physico-Chemical Characterisation	TiO_2 NM-105	ZnO NM-111	SiO_2 NM-200	$BaSO_4$ NM-220	CeO_2 NM-212
Core Composition & CAS	Titanium Dioxide CAS: 1317-80-2	Zinc Oxide CAS: 1314-13-2	Silicon Dioxide CAS: 7631-86-9	Barium Sulfate CAS: 7727-43-7	Cerium Dioxide CAS: 1306-38-3
Crystalline Phases (XRD)	86.9% Anatase + 13.1% Rutile	Zincite	Amorphous SiO_2	Barite	Cerianite
Surface Coating	N/A	Triethoxycaprylsilane	N/A	N/A	N/A
Impurities (XRF)	None (Purity >99%)	P_2O_5, SiO_2, CaO, CuO, Fe_2O_3, NiO (All <1.0%)	SO_3, Na_2O (>1%); Cl, Al_2O_3 (<1%); CaO, TiO_2, Fe_2O_3, K_2O, CuO, NiO, ZrO_2, ZnO (<0.1%)	Na, Ca, Sr, F, Cl, Organic Contaminations (Purity >93.8%)	P_2O_5, CaO, Cl (<1.0%) V_2O_5, SO_3, CoO, MgO, SiO_2, CuO, Fe_2O_3, ZnO (<0.1%)
Size (MinFeret; TEM)	25 nm	40.6 ± 26.1 nm	35.5 ± 38.9 nm	31.5 ± 15.9 nm	13.7 ± 7.6 nm
3D Aspect Ratio and Circulatory (TEM)	N/A	A.R: 1.88 ± 0.78 C: 0.80 ± 0.12	A.R: 1.57 ± 0.35 C: 0.41 ± 0.20	A.R: 1.22 ± 0.19 C: 0.98 ± 0.04	A.R: 1.21 ± 0.25 C: 0.97 ± 0.06
Surface Area (BET)	51.0 m^2/g	12.0 m^2/g	166.5 m^2/g	33.0 m^2/g	27.0 m^2/g
Density (He Pycnometer)	3.95 g/cm^3	4.99 g/cm^3	2.19 g/cm^3	4.13 g/cm^3	7.2 g/cm^3
Chemical Nature of the Surface (XPS)	Ti: 24.5% O: 65.0% C: 10.5%	Zn: 34.6% C: 22.2% O: 43.1%	C: 4.1% Na: 1.0% O: 70.8% S: 0.06% Si: 24.1%	Ba: 21.5% S: 12.5% O: 65.8%	Ce: 25.6% O: 74.4%

S5

Surface Charge (Zeta Potential at pH 7 in 10mM KCl Water Solution)	-17.0 mv	N/A	-22.0 mV	-30.2 mV	+35.2 mV
Hydrophobicity (Water Contact Angle)	Hydrophilic (60°)	Hydrophobic (152°)	Hydrophilic (<10°)	Hydrophilic (<10°)	Hydrophilic (60°)

Evaluation of dissolution rates from raw ion data

The time-resolved concentrations in the sampled eluates c_i and the fluid volume flow V_i of each sampling with duration Δt_i are evaluated towards the dissolved mass $M_{diss,\,I}$ in this sampling by correcting for the stoichiometry (Figure SI_1):

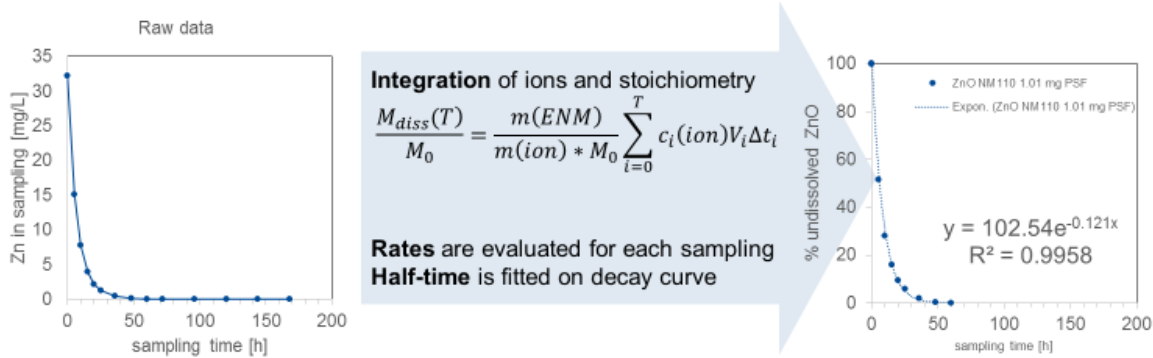$$M_{diss,i} = \frac{m(ENM)}{m(ion)} c_i(ion) V_i \Delta t_i$$

Figure SI_1: summary of calculations that are applied in the manuscript.

All dissolved mass is summed up to construct the dissolved mass fraction $M_{diss}(t)/M_0$, and the surface area at the ith sampling $SA_i(t)$. Instantaneous dissolution rates are constructed for each sampling as: $k_i = M_{diss,i}$ / SA_i / Δt_i. For slowly dissolving materials, the change of SA over time is often negligible, but for partially or quickly dissolving materials, an assumption on geometry needs to made: ISO guidance and Utembe *et al.* 2015 recommend to model the loss of solids as the shrinkage of spheres [4,5], such that the lost mass is modeled by reduced diameter: $SA(t) = BET(t=0) * [(M_0 - M_{diss}(t))/M_0]^{2/3}$. Finally, one can evaluate the dissolution results in two approaches:

- The dissolution kinetics $1-M_{diss}(t)/M_0$ can be fitted by an exponential decay to obtain the *half-time*. The half-time is a descriptor of dissolution in mass metrics with conventional unit of days.
- The *average dissolution rate k* is obtained by averaging the instantaneous rates, and is a descriptor of dissolution in surface metrics with conventional unit ng/cm²/h. Because of the uncertainties in the development of the specific surface area, only the k_i values from samplings with $M_{diss}(T) / M_0$ below 90% (i.e. more than 10% of solid mass remain) were used to calculate the average. The 10% rule has been justified by comparisons between various parameter setting [6].

The consistency between the two approaches can be checked by conversion from rate to a *calculated* half-time by $T_{\frac{1}{2}} = \frac{\ln 2}{k*BET}$, as is well-established [4].

Table SI_3: Results of particle size analysis by TEM. This data is represented in Fig.4. # particles analyzed is the total number of particles which were identified and measured for each sample.

|	Pristine ENM	Medium C: MK (phthalate)	Medium D: MG (citrate)	Medium E: MG (HCl)	Medium Muhle	Medium Midander
TiO_2 median	23	19	23	20	20	22
TiO_2 min	10	7	10	9	8	11
TiO_2 max	120	56	114	70	63	69
TiO_2 #particles analyzed	420	189	183	208	195	197
CeO_2 median	17	25	24	24	25	23
CeO_2 min	4	8	8	7	8	7
CeO_2 max	157	148	93	110	110	110
CeO_2 #particles analyzed	171	231	221	191	200	316
SiO_2 median	12	17	17	16	16	16
SiO_2 min	5	7	8	8	8	8
SiO_2 max	34	34	32	35	35	34
SiO_2 #particles analyzed	154	150	160	158	157	806
$BaSO_4$ median	18	23	21	25	28	22
$BaSO_4$ min	4	11	11	12	13	10
$BaSO_4$ max	71	40	36	36	39	28
$BaSO_4$ #particles analyzed	548	794	898	712	890	1508
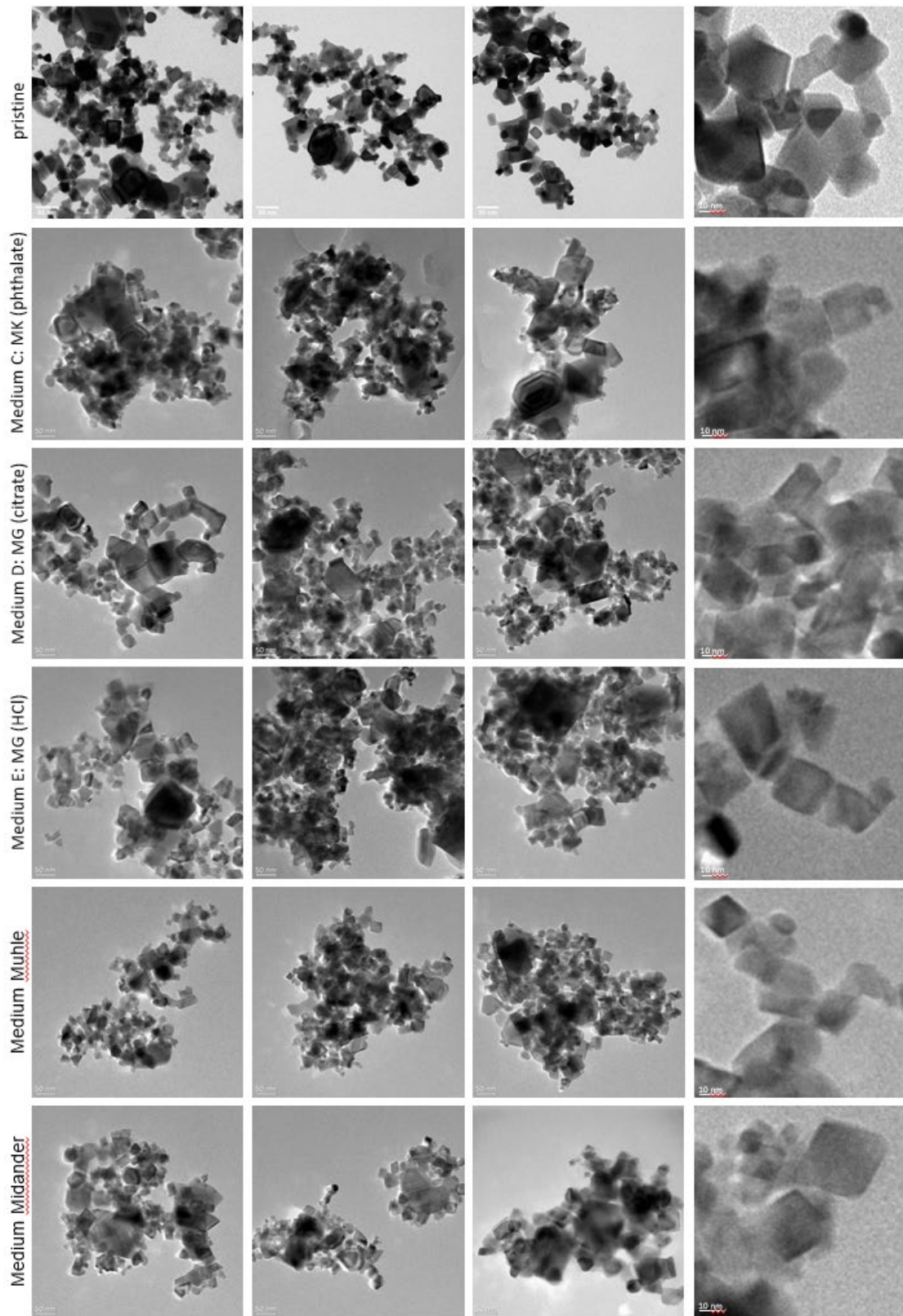
Figure SI_2: TEM re-analysis of CeO$_2$ NM-212 pristine and after 7 days of dissolution testing. For each medium, three spots on the TEM grid were imaged and evaluated.
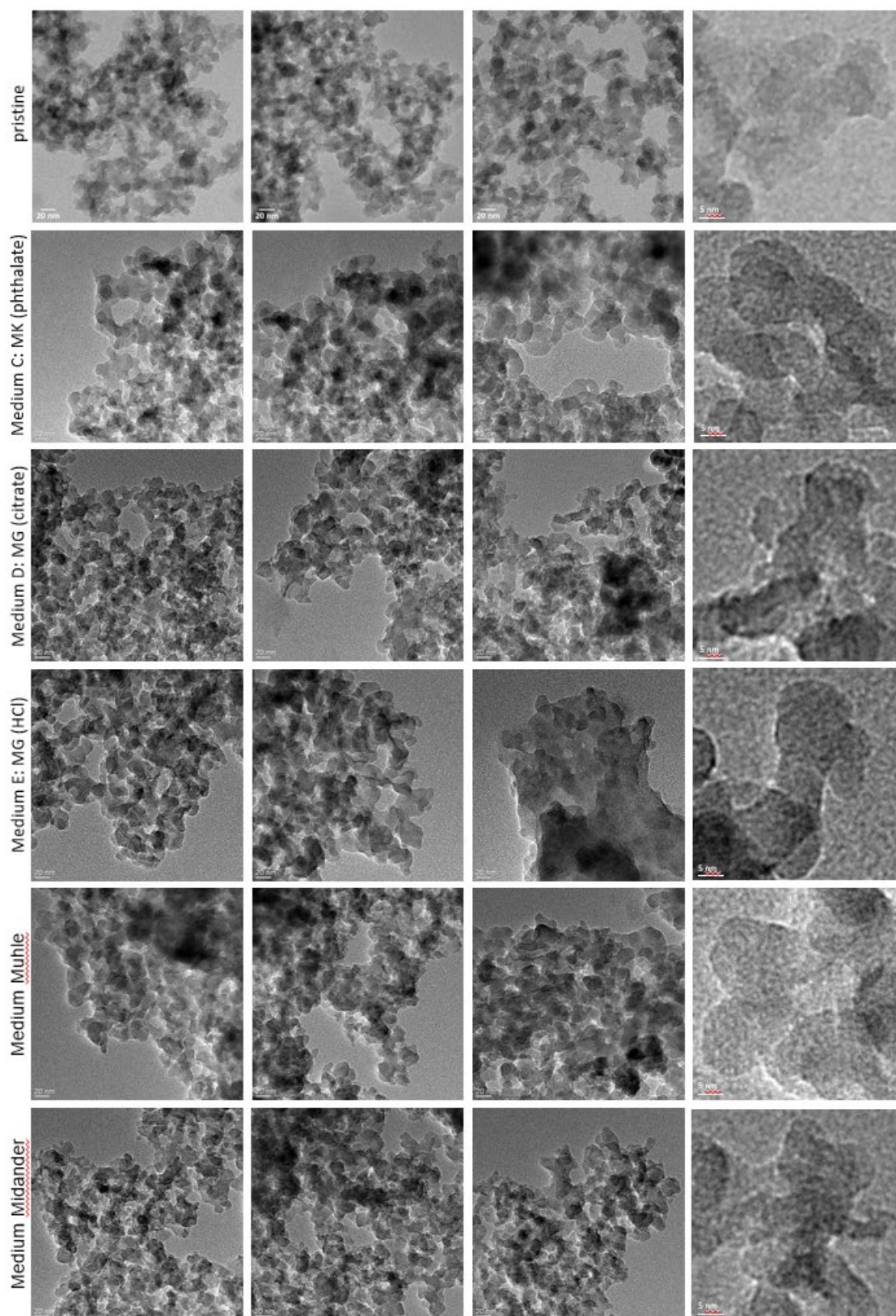
Figure SI_3: TEM re-analysis of SiO$_2$ NM-200 pristine and after 7 days of dissolution testing. For each medium, three spots on the TEM grid were imaged and evaluated.

References in the Supporting Information:

(1) PubMed.com.

(2) Sauer, U. G.; Werle, K.; Waindok, H.; Hirth, S.; Hachmöller, O.; Wohlleben, W. Critical Choices in Predicting Stone Wool Biodurability: Lysosomal Fluid Compositions and Binder Effects. *Chem. Res. Toxicol.* **2021**. https://doi.org/10.1021/acs.chemrestox.0c00401.

(3) Llewellyn, S. V.; Conway, G. E.; Zanoni, I.; Jørgensen, A. K.; Shah, U. K.; Seleci, D. A.; Keller, J. G.; Kim, J. W.; Wohlleben, W.; Jensen, K. A.; Costa, A.; Jenkins, G. J. S.; Clift, M. J. D.; Doak, S. H. Understanding the Impact of More Realistic Low-Dose, Prolonged Engineered Nanomaterial Exposure on Genotoxicity Using 3D Models of the Human Liver. *J. Nanobiotechnology* **2021**, *19* (1), 1–24. https://doi.org/10.1186/s12951-021-00938-w.

(4) Utembe, W.; Potgieter, K.; Stefaniak, A. B.; Gulumian, M. Dissolution and Biodurability: Important Parameters Needed for Risk Assessment of Nanomaterials. *Part. Fibre Toxicol.* **2015**, *12* (1), 11. https://doi.org/10.1186/s12989-015-0088-2.

(5) *ISO/TR 19057:2017 Nanotechnologies — Use and Application of Acellular in Vitro Tests and Methodologies to Assess Nanomaterial Biodurability*; 2017.

(6) Keller, J. G.; Peijnenburg, W.; Werle, K.; Landsiedel, R.; Wohlleben, W. Understanding Dissolution Rates via Continuous Flow Systems with Physiologically Relevant Metal Ion Saturation in Lysosome. *Nanomaterials* **2020**, *10* (2), 1–16. https://doi.org/10.3390/nano10020311.